Nanotechnology Perceptions
ISSN 1660-6795
www.nano-ntp.com

Two Input Powered Soft-Switched Full Bridge LED Driver with Reduced Voltage Stress

Shaik Mohammed Mukassir[1], K. Ravi Kumar[2], E. Vidya Sagar[3]

[1]Department of Electrical Engineering, Osmania University, India, mukassir_be@yahoo.com
[2]Department of Electrical and Electronics Engineering, Vasavi College of Engineering, India, k.ravikumar@staff.vce.ac.in
[3]Department of Electrical Engineering, Osmania University, India, vidyasagar.e@uceou.edu

In this research work, a full bridge converter using two input voltages for light emitting diode (LED) lighting application is proposed. Two identical LED lamps are powered. The main contributions of the proposed LED converter are: 1) switch voltage stress in full bridge is reduced; 2) zero voltage switching transition; 3) conversion power is low; 4) high converter efficiency; 5) ability to supply multiple lamps; 6) pulse-width modulation (PWM) dimming feature; 7) requires low inductor values to reduce current ripple. Across each leg of full bridge configuration, two different input voltages are connected back to back. Due to this, voltage stress of device in each leg is reduced significantly and this feature reduces the conversion power through full bridge. Input voltage connection also helps to utilize voltage and current characteristics of LEDs effectively. The steady-state operation of the proposed converter has been confirmed through numerical simulations. Additionally, an experimental prototype with an output power of 72 W has been developed to validate the simulation findings.

Keywords: Light emitting diodes, driver circuits, Resonant dc-dc converters, Zero Voltage Switching, PWM and Dimming Control.

1. Introduction

Lighting appliances utilize approximately 20% of the total electrical energy generated across the world [1-2].Thus, there is enough scope to enhance energy conservation through lighting appliances. Light emitting diode is an energy efficient light source. Most of the lighting applications are occupied by LEDs due to their characteristics such as long life, high-energy

efficiency, solid-state characteristic, faster dynamic response, and green light source, etc. [3]–[6]. Owing to their benefits, LED usage in residential, streetlight, automotive, decorative, and factory lighting systems has been increasing and expanding [7]–[9].

LED forward voltage and current characteristics are similar to the p-n junction diode [10]. Moreover, illumination output from LED depends on forward current. In many applications, the operating current of LEDs must be constant and regulated. Hence LED lighting systems are powered by constant current regulators [11-12]. They are also called LED driver circuits. Mostly switched-mode power electronic converters are used to drive LED lighting systems. Based on the availability of input supply, LEDs are powered either from ac voltage or dc voltage [13]. The requirement of ac operated LED driver and dc operated LED driver is different. In the recent past, dc power distribution has been increasing, hence dc loads can be operated separately and isolated from the utility ac grid. Thus, dc fed LED drivers have become popular in recent research topics. Further dc fed LED drivers with soft-switching features reduce the size of the lighting system greatly. Different soft-switched dc fed LED converter configurations have been proposed for lighting applications [14]-[23].

Authors in [14] presented an asymmetrical duty ratio controlled soft-switching converter to minimize the processing power for LED lighting application. LED lamps are connected across the series combination of a controlled voltage, which is produced using half-bridge series resonant inverter and unregulated dc voltage. Parallel LED lamps are regulated using controlled voltage. However independent pulse-width modulation (PWM) dimming of lamps is addressed with extra switching devices. A half bridge based soft-switched converter using three controlled switches is presented to drive two different LED lamps [15]. Lamp current regulation and PWM dimming feature are achieved independently. However, switching logic for independent control requires an additional circuit and component count per lamp is comparable. In [16], two identical lamps are powered using three leg full bridge converters. To improve conversion efficiency, each lamp has a dc voltage in series. Two full bridge converters with one common leg produce asymmetrical voltage, which helps to achieve lamp current regulation. Further, both lamps are dimmed using pulse-width modulation independently. Input-modulated full bridge driver circuits with the soft-switching feature are presented to power multiple identical LED lamps [17]-[18]. However independent relation and dimming are not addressed. Buck-boost integrated half-bridge series resonant converter with high gain [19] is proposed solar/battery powered LED lighting applications. Regulation using variable frequency, zero-voltage switching (ZVS), PWM illumination control, extension of configuration to multiple LED lamps are some of the claims in this study. In [20], two LED lamps with different wattages are supplied from coupled inductor-based driver circuits with soft-switching. In this paper, leakage energy is used to power one LED lamp which limits its rating. A half-bridge based zero voltage switching converter without resonant capacitor is proposed to supply multiple LED lamps in [21]. Independent regulation, dimming, ZVS feature, etc. are achieved. However variable inductor design and implementation require additional control circuits. A combination of half and full bridge resonant converter is used to power two different LED lamps independently [22]. It features independent operation, dimming, and regulation. But the current stress of devices in the common leg is high and also their ZVS feature is not complete. Class-E resonant converter [23] with modification is used as a current regulator for LED lamp.

This research paper proposes a full bridge converter with two input voltages to power two identical LED lamps. The two input voltages are connected in anti-series configuration. This feature reduces the voltage across each switch in full bridge. This topology provides zero voltage switching, low conversion power, PWM dimming, high energy efficiency. This study is organized as follows. Section 2 presents the description and operating principle of the proposed LED driver. Steady state analysis is given in Section 3. Section 4 describes the design procedure. Simulation and experimental results are presented in Section 5 and conclusions are given in Section 6.

2. Description and Operating Principle of the Proposed LED Driver

Figure 1 illustrates the proposed LED driver with a two-input soft-switched full bridge configuration. The first leg of the full bridge is comprised of two power MOSFETs (Q_1 & Q_2), while leg-2 consists of two power MOSFETs (Q_3 & Q_4). A parasitic body diode and capacitance are included with each MOSFET switch. The input dc voltages, V_{dc1} and V_{dc2}, are connected in anti-series with the midpoint terminal 'O' across each leg. Point A represents the midpoint of leg-1, while point B represents the midpoint of leg-2. To the midpoints of leg-1 and leg-2, a series LC tank circuit, which is a series combination of resonant inductor (L_r) and capacitor (C_r) is connected. Voltage across tank circuit is represented as v_{AB}. This LED driver circuit supplies two similar rating LED lamps. Inductor L_1 and LED lamp-1 are connected in series between terminal A and O, while inductor L_2 and LED lamp-2 are connected in series between terminal B and O. Inductors L_1 and L_2 are employed to minimize the current ripple in lamp-1 and lamp-2, respectively. V_{01} and i_{01} represent the output voltage and current of lamp-1, while V_{02} and i_{02} indicate the output voltage and current of lamp-2. A switch Q_d is connected in series with input voltage V_{dc1} and it is used to achieve PWM dimming operation of both lamps. Gate voltages for switches and the operating waveforms of the proposed configuration are shown in Figure 2. Switches (Q_1 – Q_4) in full bridge operate at switching period (T). Gate voltages of Q_1 and Q_4 are given for D_1T duration and Q_2 and Q_3 are for D_3T duration. Between D_1T and D_3T durations, two dead time intervals (t_{d1} & t_{d2}) are introduced in every switching cycle to protect switches in full bridge. The operation of proposed topology is described in four modes over a time period (T). The equivalent circuit in each mode with current direction are shown in Figure 3 and 4.

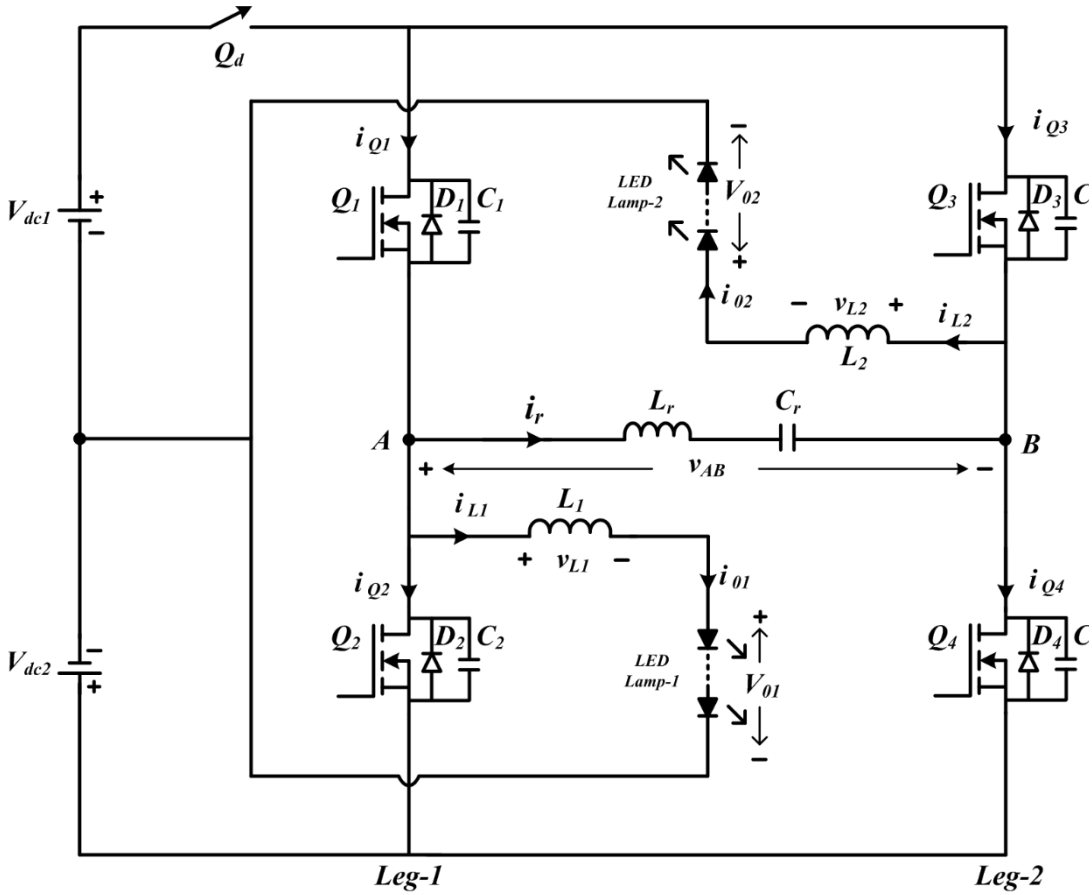

Figure 1. Power circuit illustration of proposed configuration.

2.1 Mode-1

This mode starts after giving gate voltages (v_{g1} & v_{g4}) to upper switch (Q_1) in leg-1 and bottom switch (Q_4) in leg-2 at time t = t_0. Figure 3 (a) shows the operative equivalent circuit. From t_0 – t_1, switches Q_1 & Q_4 allow the currents through them. The voltage (v_{AB}) across resonant tank circuit is $+(V_{dc1} - V_{dc2})$. Consequently, a resonant current, i_r passes through Q_1 & Q_4. During this state, the voltage across L_1 is $(V_{dc1} - V_{01})$. As a result, inductor L_1 accumulates energy as the current (i_{L1}) through Q_1 linearly increases. Similarly, voltage across L_2 is $(V_{dc2} - V_{02})$, hence inductor L_2 releases energy as the current (i_{L2}) through Q_4 linearly decreases. The sum of i_r and i_{L1} flows through switch Q_1 and difference of i_r and i_{L1} flows in Q_4. At t = t_1, gate control voltage (v_{g1} & v_{g4}) are removed and mode-1 is stopped.

2.2 Mode-2

The mode-2 duration is from t = t_1 to t = t_2. The operative equivalent is shown in Figure 3(b). No switch is conducting in this mode. However, the inductive currents in the previous mode cannot change their directions instantaneously. Thus, switch parasitic capacitances (C_1 – C_4)

allow these currents. The turn-off process of switches Q_1 and Q_4 is initiated at $t = t_1$ and voltage across C_1 and C_4 are zero. The switches Q_2 and Q_3 are still in the off state, with their parasitic capacitances C_2 and C_3 being charged to $(V_{dc1} - V_{dc2})$. In leg-1 from $t = t_1$ to $t = t_2$, the drain to source capacitance C_1 allows a current of $(i_r+i_{L1})/2$ and hence it start charging from zero to $(V_{dc1} - V_{dc2})$. And, C_2 is discharged from $(V_{dc1} - V_{dc2})$ to zero by $(i_r+i_{L1})/2$, while in leg-2, C_3 is discharged from $(V_{dc1} - V_{dc2})$ to zero by current $(i_r - i_{L2})/2$. When voltage across body diodes of Q_2 and Q_3 is -0.7 V, gate voltages (v_{g2} & v_{g3}) will be applied to devices Q_2 and Q_3 for zero voltage switching-on transition. At $t = t_2$, mode-3 is initiated.

2.3 Mode-3

This mode starts after giving gate voltages (v_{g2} & v_{g3}) to bottom switch (Q_2) in leg-1 and upper switch (Q_3) in leg-2 at time $t = t_2$. Figure 4 (a) shows the operative equivalent circuit. From $t_2 - t_3$, switches Q_2 & Q_3 allow different currents through them. The voltage (v_{AB}) across resonant tank is $-(V_{dc1} - V_{dc2})$. As a result, a resonant current, i_r is conducted through switches Q_2 & Q_3. In this mode, the voltage across L_1 becomes negative, resulting in a linear decrease in i_{L1} through Q_2. Simultaneously, current in L_2 rises linearly through Q_3 due to the voltage across L_2, which is $(V_{dc1} - V_{02})$. Switch Q_2 conduct the difference of resonant current i_r and i_{L1} and Q_3 sum of i_r and i_{L2}. This mode terminates at $t = t_3$.

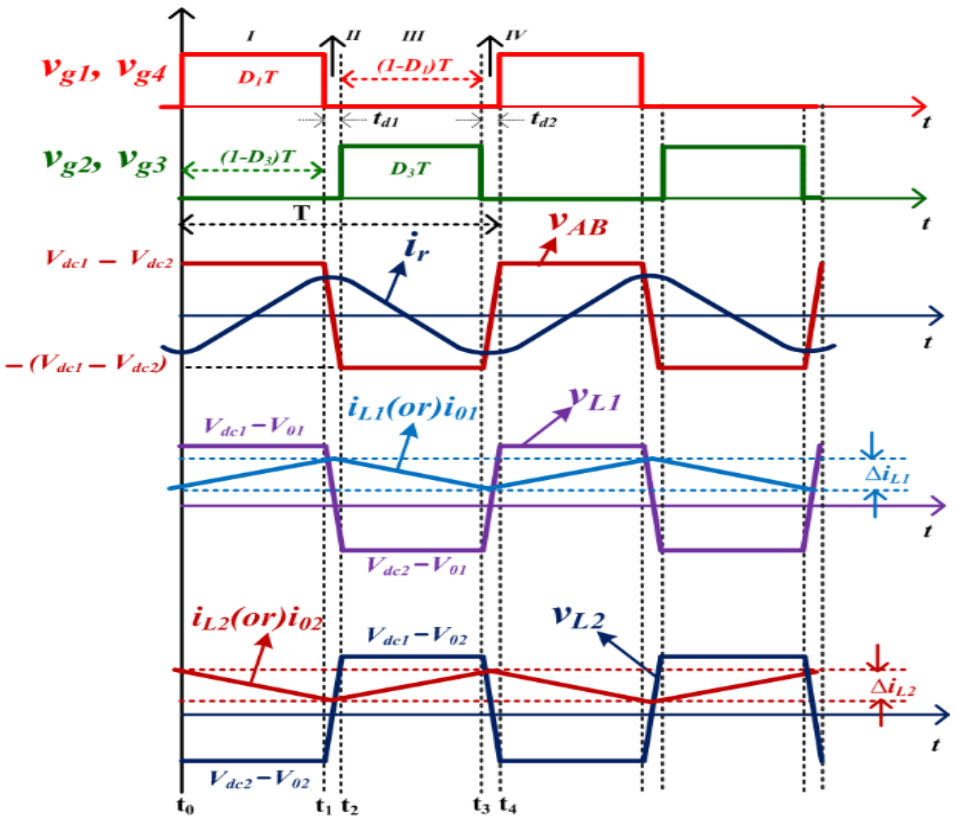

Figure 2. Operating waveforms

2.4 Mode-4

During t_3 to t_4, devices Q_2 and Q_3 complete zero voltage turn-off transition and Q_1 & Q_4 complete zero voltage turn-on transition. This switching transition process is similar to that given in mode-2. Figure 4(b) shows the operative equivalent circuit with no switch conducting. At $t = t_4$, the switching cycle is completed.

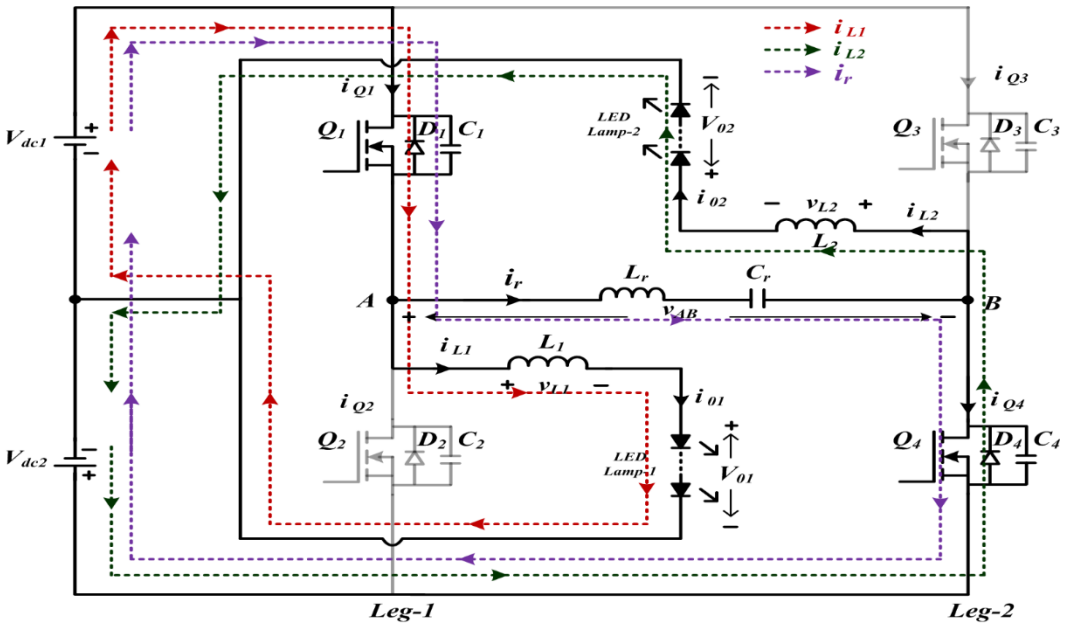

Figure 3 (a) Operative equivalent circuit in mode-1

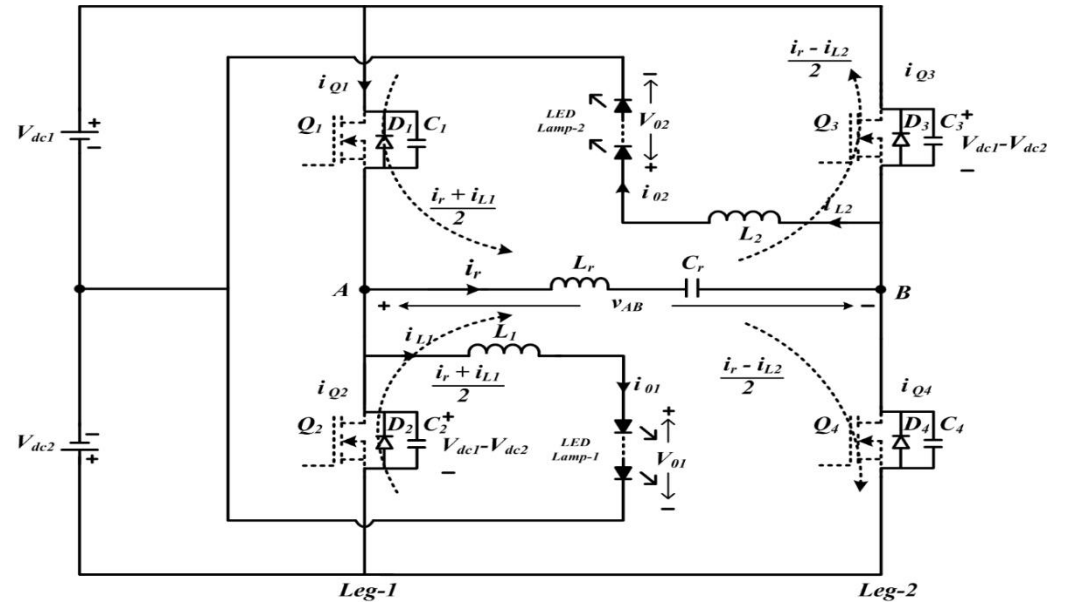

Figure 3 (b) Operative equivalent circuit in mode-2

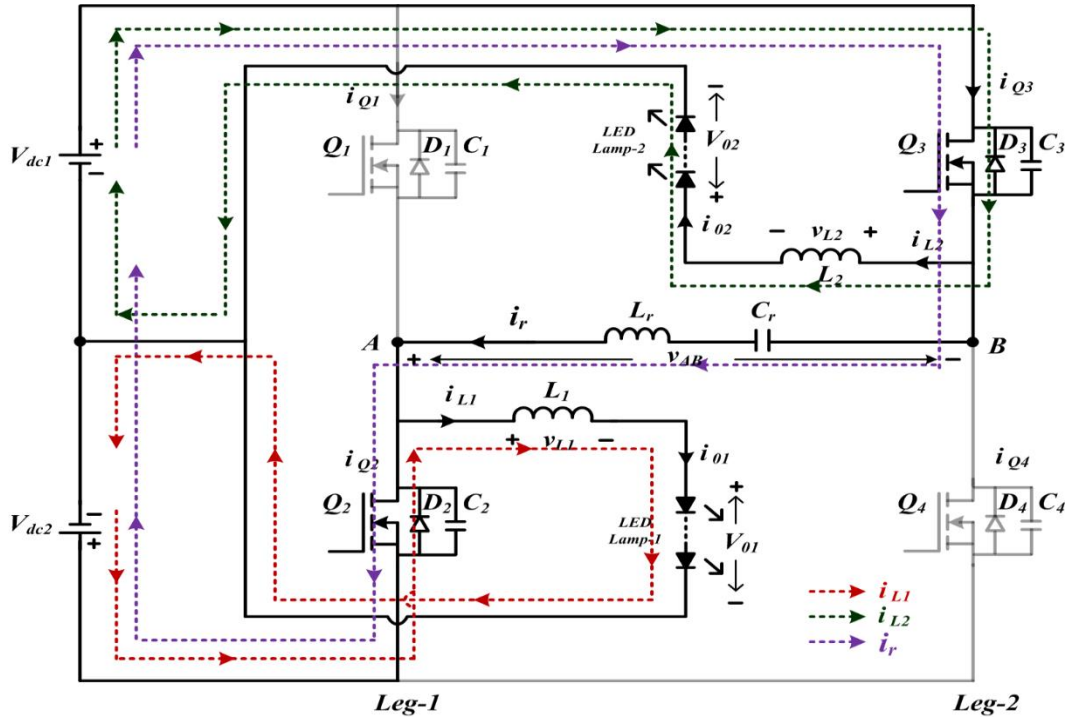

Figure 4 (a) Operative equivalent circuit in mode-3

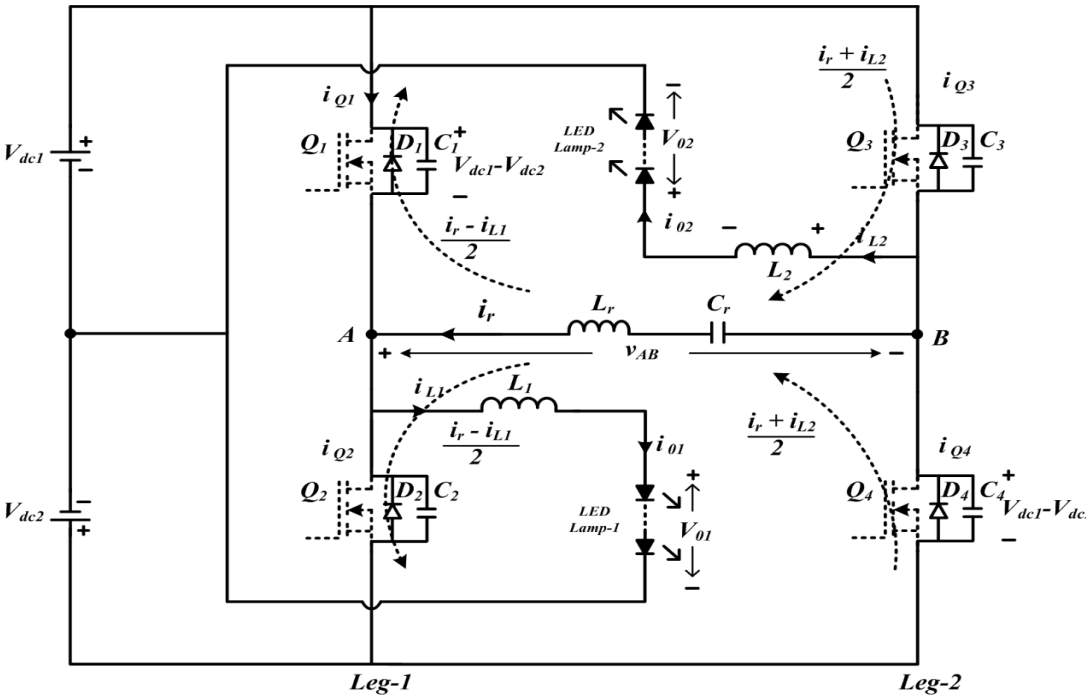

Figure 4 (b) Operative equivalent circuit in mode-4

3. Steady State Analysis

To derive steady state input and output voltage relation of the proposed configuration, the below considerations are made.

(i) All the passive elements and semi-conductor devices are lossless.

(ii) Voltage across each LED lamp is constant with no ripple.

(iii) Input dc voltage, V_{dc1} < input dc voltage V_{dc2} < output voltage, V_{01} & V_{02}

The analysis is carried out by neglecting dead times in a switching cycle. To write voltage and current relations in mode-1, the circuit depicted in Figure 3(a) is considered. D_1T is the ON duration of switch Q_1 and Q_4. $(1\text{-}D_3)T$ is OFF duration of switch Q_2 and Q_3. When the switch Q_1 & Q_4 are ON,

The voltage and current in inductor L_1 are given by

$$v_{L1} = V_{dc1} - V_{01} = L_1 \frac{di_{L1}}{dt} \qquad t_0 \le t < t_1 \tag{1}$$

$$i_{L1}(t) = \frac{1}{L_1}\int_{t_0}^{t} v_{L1}(t)dt + i_{L1}(t_0) \qquad t_0 \le t < t_1 \tag{2}$$
$$= \frac{V_{dc1} - V_{01}}{L_1}(t - t_0) + i_{L1}(t_0)$$

$i_{L1}(t_0)$ represents the initial current at time $t = t_0$ in inductor (L_1). The maximum current through L_1 is written as

$$i_{L1}(t_1) = \frac{V_{dc1} - V_{01}}{L_1}(t_1 - t_0) + i_{L1}(t_0) \tag{3}$$

Where the duration $(t_1 - t_0)$ is the conduction duration of Q_1. Hence equation (3) is modified as

$$i_{L1}(t_1) = i_{L1}(t_0) + \frac{V_{dc1} - V_{01}}{L_1} D_1 T \tag{4}$$

The peak-peak current ripple in L_1 is specified from equation (4) as

$$\Delta i_{L1} = i_{L1}(t_1) - i_{L1}(t_0) = \frac{V_{dc1} - V_{01}}{L_1} D_1 T \tag{5}$$

Similarly, LED lamp-2 is supplied by the stored energy in inductor L_2 through switch Q_4.

The voltage and current in inductor L_2 are given by

$$v_{L2} = V_{dc2} - V_{02} = L_2 \frac{di_{L2}}{dt} \qquad t_0 \le t < t_1 \tag{6}$$

$$i_{L2}(t) = i_{L2}(t_0) + \frac{1}{L_2}\int_{t_0}^{t} v_{L2}(t)dt = i_{L2}(t_0) + \frac{V_{dc2} - V_{02}}{L_2}(t - t_0) \qquad t_0 \le t < t_1 \qquad (7)$$

$i_{L2}(t_0)$ represents the initial current at time $t = t_0$ in inductor (L_2). The maximum current through L_2 is written as

$$i_{L2}(t_1) = i_{L2}(t_0) + \frac{V_{dc2} - V_{02}}{L_2}(t_1 - t_0) \qquad (8)$$

Where $(t_1 - t_0)$ duration is the non-conducting duration of switch Q_3. It can be written as follows

$$i_{L2}(t_1) = i_{L2}(t_0) + \frac{V_{dc2} - V_{02}}{L_2}(1 - D_3)T \qquad (9)$$

From equation (9), the peak-peak current ripple in inductor L_2 is specified as

$$\Delta i_{L2} = i_{L2}(t_1) - i_{L2}(t_0) = \frac{V_{dc2} - V_{02}}{L_2}(1 - D_3)T \qquad (10)$$

During $t_1 - t_0$, the voltage (v_{AB}) across resonant tank is $+(V_{dc1} - V_{dc2})$. The resonant current in tank circuit is given as

$$i_r(t) = \frac{v_{AB}}{Z_0}\sin\omega_0(t - t_0) + i_r(t_0)$$
$$= +(V_{dc1} - V_{dc2})\sqrt{\frac{C_r}{L_r}}\sin\omega_0(t - t_0) + i_r(t_0) \qquad t_0 \le t < t_1 \qquad (11)$$

Where Z_0 = Characteristic Impedance = $\sqrt{\frac{L_r}{C_r}}$;

$\omega_0 = \frac{1}{\sqrt{L_r C_r}}$ = Resonant Frequency

When the switches Q_2 & Q_3 are ON, the voltage and current in inductor L_1 are given by

$$v_{L1} = V_{dc2} - V_{01} = L_1\frac{di_{L1}}{dt} \qquad t_2 \le t < t_3 \qquad (12)$$

$$i_{L1}(t) = \frac{1}{L_1}\int_{t_2}^{t} v_{L1}(t)dt + i_{L1}(t_2) = \frac{V_{dc2} - V_{01}}{L_1}(t - t_2) + i_{L1}(t_2) \qquad t_2 \le t < t_3 \quad (13)$$

The voltage and current in inductor L_2 are given by

$$v_{L2} = V_{dc1} - V_{02} = L_2 \frac{di_{L2}}{dt} \qquad t_2 \le t < t_3 \tag{14}$$

$$i_{L2}(t) = i_{L2}(t_2) + \frac{V_{dc1} - V_{02}}{L_2}(t - t_2) \qquad t_2 \le t < t_3 \tag{15}$$

The magnitude of ripple current in inductor L_1 and L_2 are given by

$$\Delta i_{L1} = i_{L1}(t_3) - i_{L1}(t_2) = \frac{V_{dc2} - V_{01}}{L_1}(1 - D_1)T \tag{16}$$

$$\Delta i_{L2} = i_{L2}(t_3) - i_{L2}(t_2) = \frac{V_{dc1} - V_{02}}{L_2} D_3 T \tag{17}$$

During t_2 –t_3, the voltage (v_{AB}) across resonant tank circuit is $-(V_{dc1} - V_{dc2})$. Hence the current through it is expressed as

$$\begin{aligned} i_r(t) &= i_r(t_2) + \frac{v_{AB}}{Z_0} \sin \omega_0 (t - t_2) \\ &= i_r(t_2) - (V_{dc1} - V_{dc2}) \sqrt{\frac{C_r}{L_r}} \sin \omega_0 (t - t_2) \end{aligned} \qquad t_2 \le t < t_3 \tag{18}$$

For steady state operation, volt-sec balance in inductor L_1 is used to derive the output voltage of LED lamp-2. Therefore from (1), (12), V_{01} is obtained as

$$\frac{V_{dc1} - V_{01}}{L_1} D_1 T + \frac{V_{dc2} - V_{01}}{L_1}(1 - D_1)T = 0$$

$$V_{01} = V_{dc2} + D_1 (V_{dc1} - V_{dc2}) \tag{19}$$

Similarly, by applying volt-sec balance in inductor L_2, output voltage of lamp-2 is obtained as

$$V_{01} = V_{dc2} + D_3 (V_{dc1} - V_{dc2}) \tag{20}$$

4. Design Analysis

In the proposed topology, LED lamp-1 and inductor L_1 are connected in series between the midpoint of leg-1 and the midpoint of the anti-series input DC voltages. Similarly, LED lamp-2 and inductor L_2 are connected in series between the midpoint of leg-2 and the midpoint of the anti-series input DC voltages. The rating of lamp-1, lamp-2, calculation of (L_1 & L_2), calculation of (L_r & C_r) and input voltage are presented in section. LED equivalent circuit [24] is required to determine the parameters related to lamp-1 and lamp-2. TMX HP 3WLEDs are utilized in this study. The voltage-current characteristics of used LEDs are illustrated in Figure 5. It is observed that LED starts conduction from the threshold voltage (V_{th}) of 2.3 V, and an operating point at a forward voltage (V_F) of 3.25 V and a forward current (I_F) of 510 mA is

selected. The proposed converter employs two LED lamps, each consisting of two strings with 11 LEDs connected in series in each string. Consequently, threshold voltage of each lamp is determined to be 25.3 V and each lamp operates at 1.02 A, 35.75 V and 36 W. The output voltage (V_{01} & V_{02}) of both lamps are measured at 35.75 V, and output currents (i_{01} & i_{02}) are at 1.02 A. In output expression of V_{01}, V_{dc2} is in series with $D_1(V_{dc1} - V_{dc2})$. Therefore V_{dc2} is selected as 24 V, as it is below the lamp's threshold voltage. The full bridge converter supplies the remaining 11.75 V to LED lamp.

According to equation (19), the input dc voltage V_{dc1} is represented as.

$$V_{dc1} = V_{dc2} + \frac{V_{01} - V_{dc2}}{D_1} \quad (21)$$

With a V_{01} of 35.75 V, a duty ratio (D_1) of 0.5, and V_{dc2} of 24 V, V_{dc1} is calculated by

$$V_{dc1} = \frac{35.75 - 24}{0.5} + 24 \cong 48V$$

The values of inductor L_1 and L_2 are calculated using equation (5) and (17) respectively.

With a switching frequency of 100 kHz, D_1 of 0.5, V_{dc2} of 24 V, V_{dc1} of 48 V. V_{01} of 35.75 V, and Δi_{L1} is 10% of i_{01}, from equation (5), the value of inductor L_1 can be determined as

$$L_1 = \frac{V_{dc1} - V_{01}}{\Delta i_{L1}} D_1 T = \frac{(48 - 35.75)}{(0.1 \times 1.02)} \cdot (0.5) \cdot 10 \cdot 10^{-6} \cong 600 \mu \text{H}$$

Similarly, with a switching frequency of 100 kHz, D_3 of 0.5, V_{dc2} of 24 V, V_{dc1} of 48 V. V_{01} of 35.75 V, Δi_{L2} is 10% of i_{02}, from equation (17), the inductor L_2 is calculated as

$$L_2 = \frac{V_{dc1} - V_{02}}{\Delta i_{L2}} D_3 T = \frac{(48 - 35.75)}{(0.1 \times 1.02)} \cdot (0.5) \cdot 10 \cdot 10^{-6} \cong 600 \mu \text{H}$$

In the proposed configuration, two lamps are supplied using a full bridge configuration. In every switching cycle, devices in full bridge do not conduct during dead time (t_{d1} and t_{d2}) intervals. Dead times between top and bottom device in each leg are expected in bridge configurations to avoid dead short circuit across input voltage. However, these dead times are also utilized to achieve zero voltage turn on and off switching transitions. No switch is conducting during t_{d1} and t_{d2}, but device parasitic capacitors ($C_1 - C_4$) carry the currents, which assist in achieving zero-voltage switching transitions in switches Q_1 to Q_4 within the full bridge circuit. Current in LC resonant tank circuit helps to achieve soft-switching during the dead time interval. Therefore, a resonant frequency of 79.62 kHz has been chosen. The resonant frequency of the full bridge can be calculated using the formula,

$$f_r = \frac{1}{2\pi\sqrt{L_r C_r}} \quad (22)$$

The capacitance value (C_r) chosen is 47 nF. According to equation (22), L_r is determined to be 85 uH.

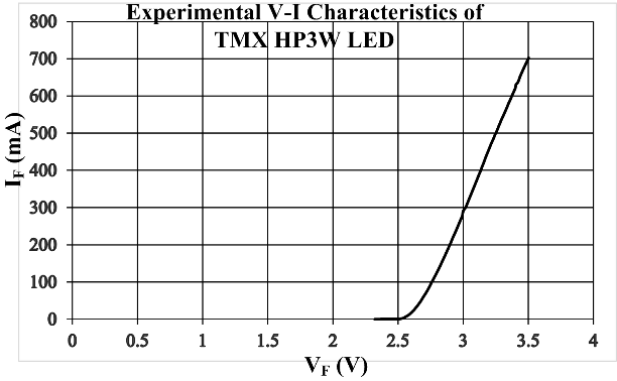

Figure 5. Voltage and current characteristics of TMX HP 3WLED

Table 1 Parameters of the proposed LED driver

DC input voltage, V_{dc1}	48 V
DC input voltage, V_{dc2}	24 V
Switching frequency, f_s	100 kHz
Resonant frequency, f_0	79.62 kHz
Resonant inductor, L_r	85 µH
Resonant capacitor C_r	47 nF
Inductor, $L_{1,2}$	600 µH
Current in lamp-1 and lamp-2, i_{01} (or) i_{02}	1.02 A
Lamp-1 and lamp-2 voltage, $V_{01,02}$	35.75 V
$P_{01,02}$	36 W
Switching devices used	IRF 640N

5. Simulation and Experimental Results

The simulation and experimental results of the proposed two input LED driver configuration are discussed in this section. The table 1 presents the voltage, current, and power ratings, as well as the component values for the LED lamp. The proposed two-input configuration is designed to power two lamps of total 72 W. Numerical simulations are conducted using OrCAD PSpice software and also validated through experimental prototype. At rated illumination, simulation and experimental waveforms of switch gate voltages (v_{g1} – v_{g4}),

voltage and current in resonant tank are shown in Figure 6. It is observed that switch gate voltages ($v_{g1} - v_{g4}$) are switched at 100 kHz with equal duty ratio, resulting in bridge output voltage (v_{AB}) of $\pm(V_{DC1} - V_{DC2})$ magnitude and resonant current with triangular in nature flows. Figure 7 presents simulated and experimental voltage and current waveforms for both lamps and they are operated at selected values. It is observed that voltage and current in lamp-1 and lamp-2 are identical. Simulation and experimental switching waveforms for switches in leg-1 are shown in Figure 8. It is observed that the devices in leg-1 complete switching transitions at zero voltage within the specified dead time between v_{g1} and v_{g2}. In Figure 9, voltage and current in both inductors (L_1 & L_2) are shown. It is observed that voltage across both the inductors is low and based on their polarity inductors are charged or discharged. At rated power, the efficiency of the proposed soft-switched LED driver is found to be 92.24%.

To incorporate dimming feature of lamp currents in the proposed two input configuration, a switch Q_d is connected in series with input voltage and it operates at 100 Hz frequency. It totally turns ON and OFF all the lamps at selected operating current. Figure 10 illustrates the dimming waveforms of the lamps, with lamp voltage and currents at 80%, 60%, and 40% dimming levels in Figures 10 (a), (b), and (c) respectively. It clearly indicates lamps are at selected current magnitudes and their illumination is controlled by PWM dimming scheme. The efficiency of proposed configuration at 80%, 60% and 40% dimming conditions are calculated to be 92.15%, 92.4% and 91.86% respectively.

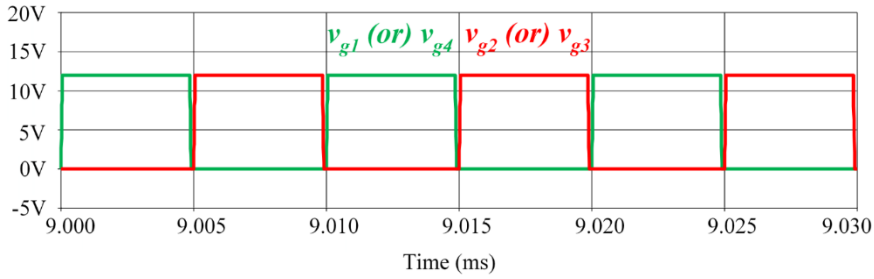

(a) Simulation waveforms of $v_{g1} - v_{g4}$.

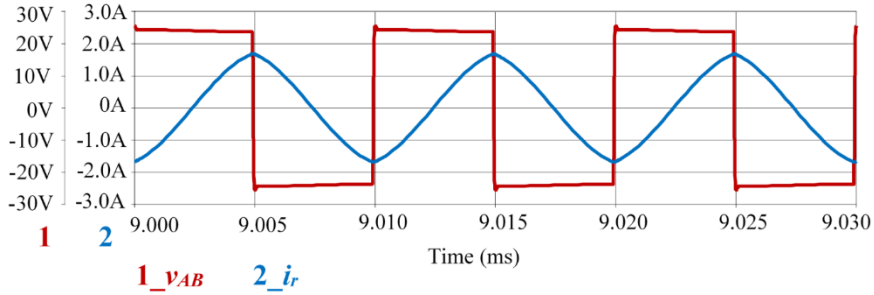

(b) Simulation waveforms v_{AB} and i_r

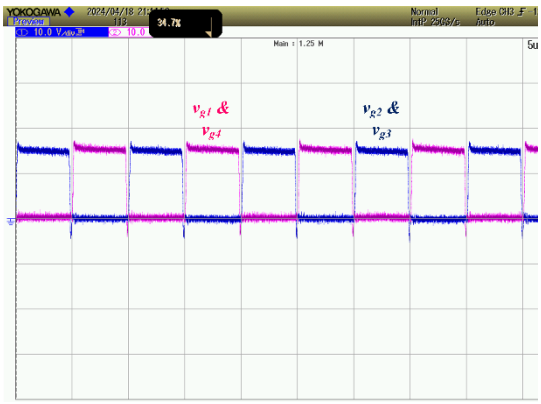

(c) Experimental waveforms of $v_{g1} - v_{g4}$.

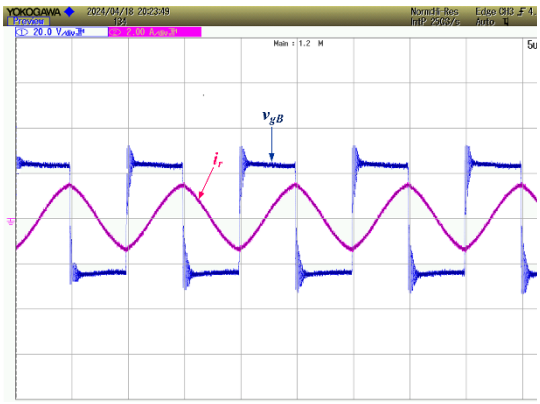

(d) Experimental waveforms v_{AB} and i_r

Figure 6. Simulation and experimental waveforms of gate voltages of switches, output voltage of full bridge and resonant current.

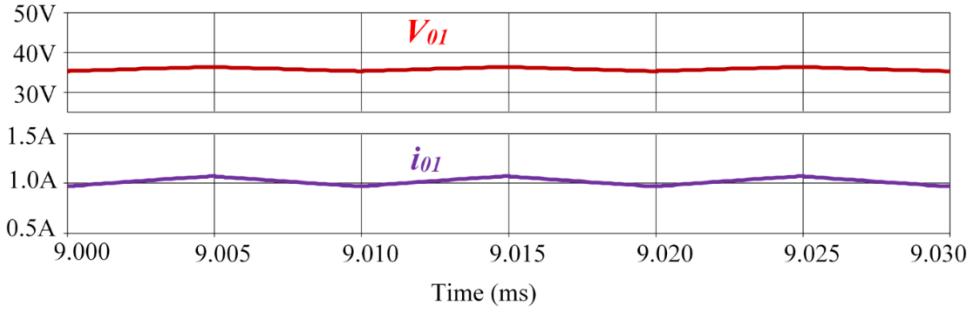

(a) V_{01} and i_{01} from simulation

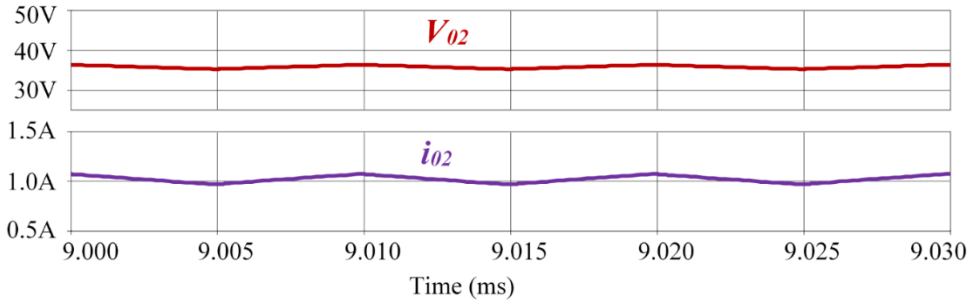

(b) V_{02} and i_{02} from simulation

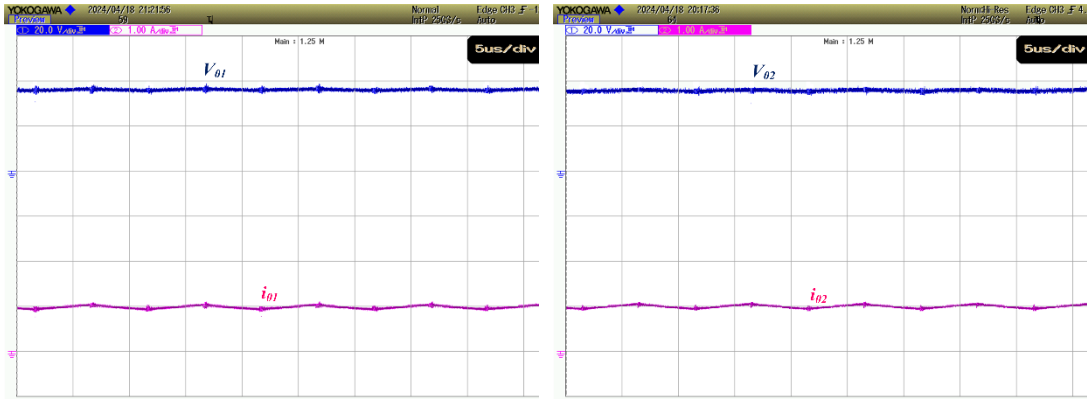

(c) V_{01} and i_{01} from experiment (d) V_{02} and i_{02} from experiment

Figure 7. Simulated and experimental waveforms of voltage and current in LED lamp-1 and LED lamp-2

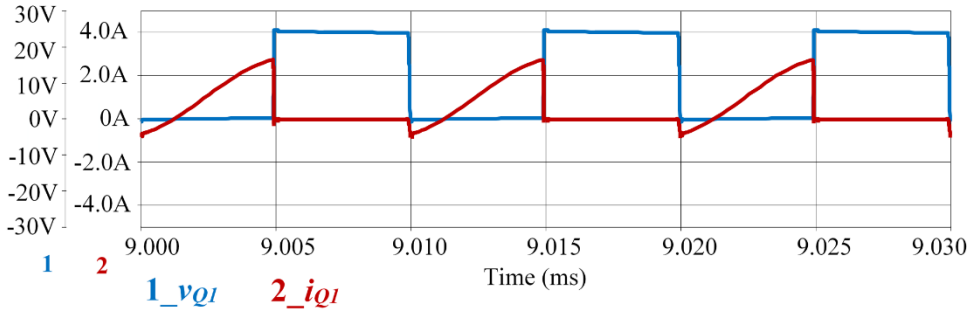

(a) Voltage and current waveforms in Q_1 from simulation

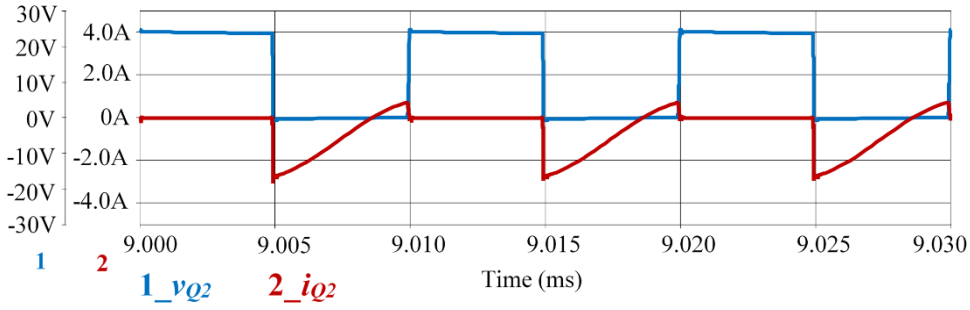

(b) Voltage and current waveforms in Q_2 from simulation

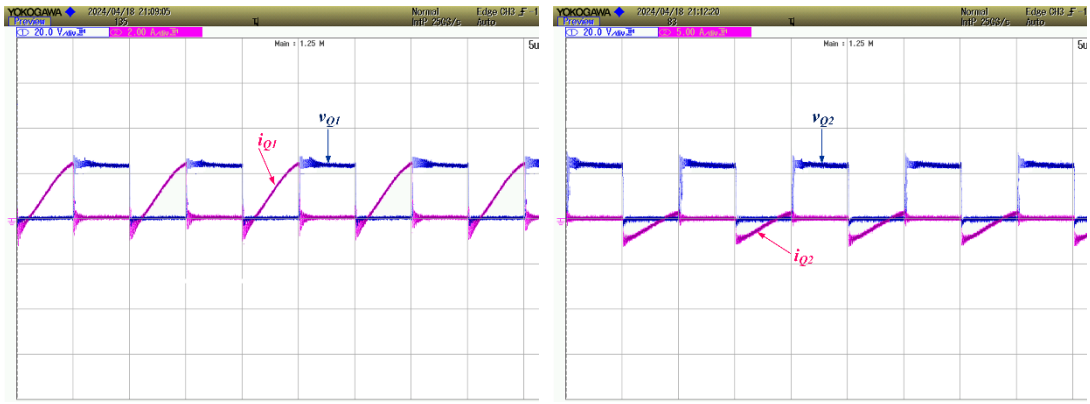

(c) Voltage and current waveforms in Q_1 from experiment

(d) Voltage and current waveforms in Q_2 from experiment

Figure 8. Simulation and experimental switching waveforms for switches in leg-1.

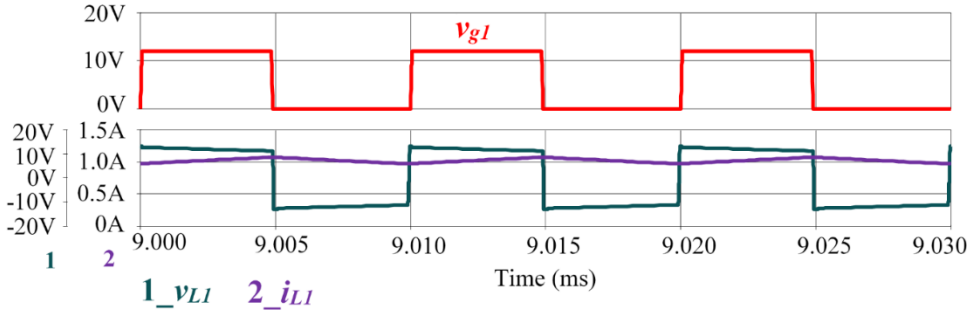

(a) Simulation waveforms of gate voltage (v_{g1}), voltage across and current in L_1

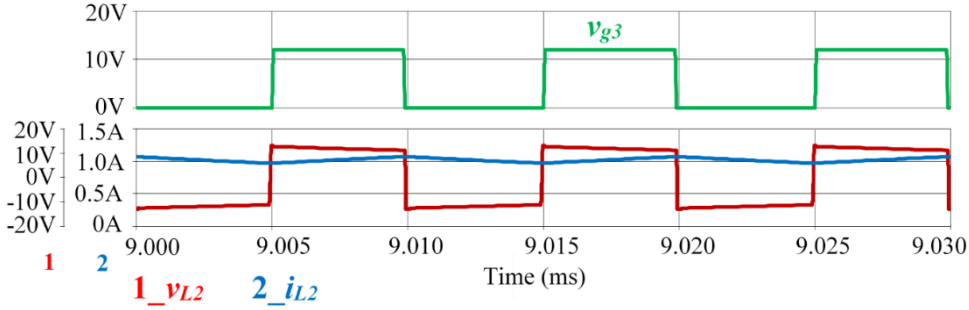

(b) Simulation waveforms of gate voltage (v_{g3}), voltage across and current in L_2

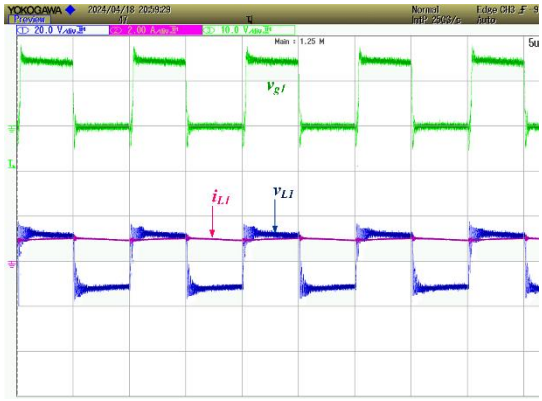

(c) Experimental waveforms of gate voltage (v_{g1}), voltage across and current in L_1

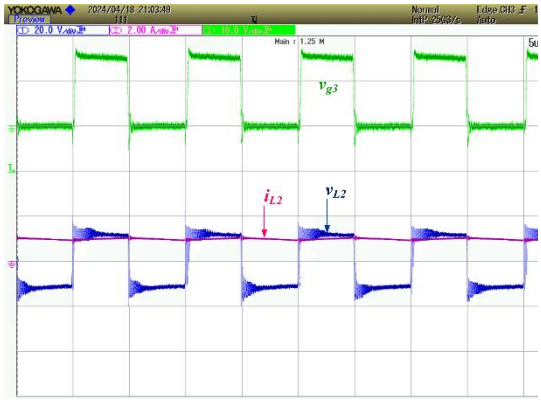

(d) Experimental waveforms of gate voltage (v_{g3}), voltage across and current in L_2

Figure 9. Simulation and experimental waveforms of voltage and current in both inductors (L_1 & L_2).

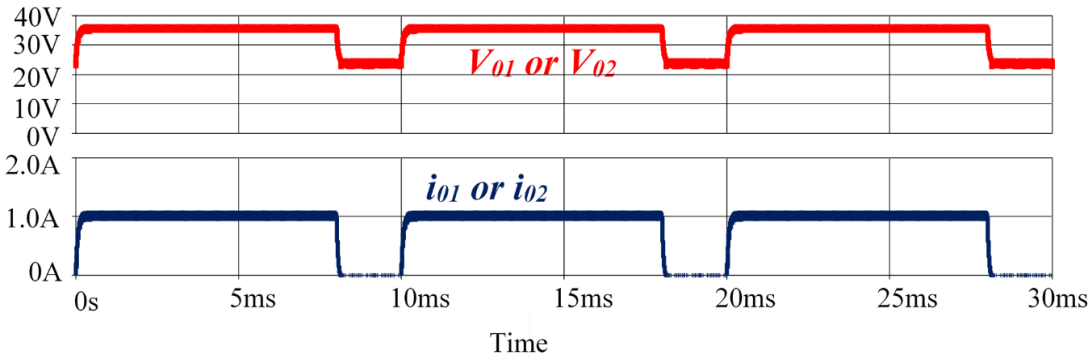

(a) Lamp currents at 80% dimming

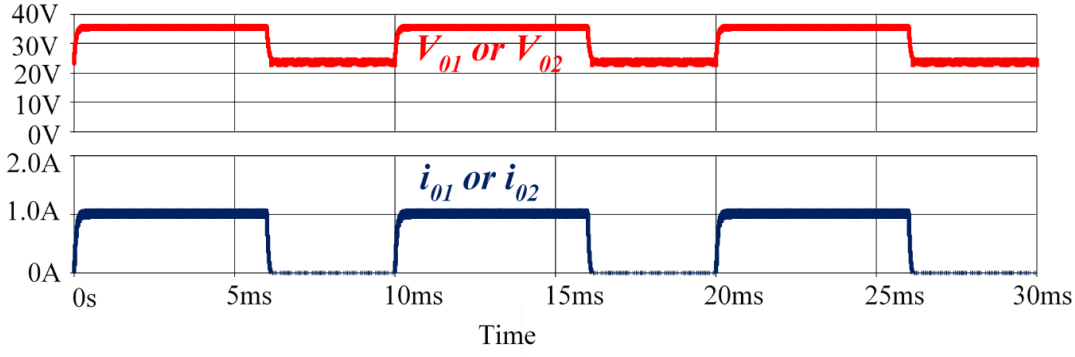

(b) Lamp currents at 60% dimming

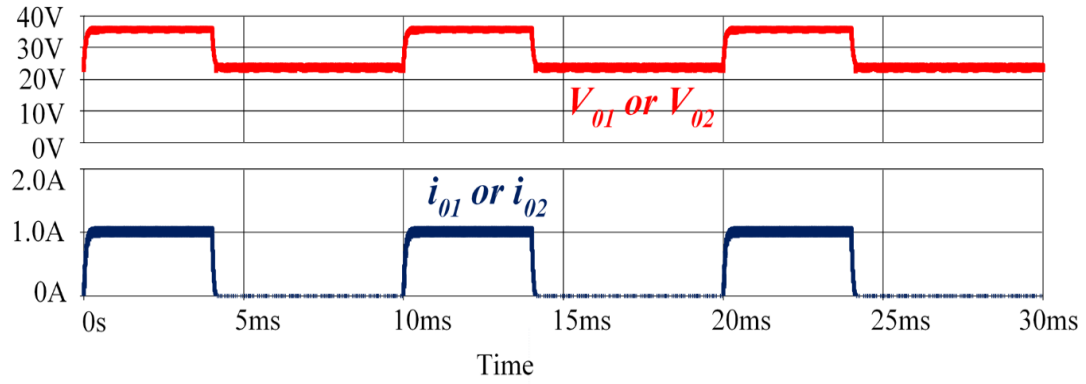

(c) Lamp currents at 40% dimming

Figure 10. Dimming waveforms.

6. Conclusion

This research study introduces a two-input powered full bridge converter that aims to reduce voltage stress in order to power two LED lamps. It details operating principle with different modes, analysis, design procedures, simulations, and experimental results. The key benefits of the proposed configuration are: i) reduced power processing ii) voltage across switches in full bridge is low, iii) zero-voltage switching characteristic, iv) high conversion efficiency, v) PWM dimming operation, and 6) ability to supply multiple lamps. The voltage across switches in full bridge is determined by the anti-series input voltages. Additionally, a 72 W experimental prototype was developed to validate numerical simulations. This configuration may be operated from future DC-grid to suit various lighting systems in factories, loco sheds, and main office buildings, etc.

References

1. U. Ramanjaneya Reddy and B. L. Narasimharaju, “Single-stage electrolytic capacitor less non-inverting buck-boost pfc based ac–dc ripple free led driver,” IET Power Electronics, vol. 10, no. 1, pp. 38–46, 2017.
2. Ch, Kasi, PorpandiselviShunmugam and Vishwanathan Neti. An efficient full-bridge resonant converter for light-emitting diode (LED) application with simple current control. International Journal of Circuit Theory and Applications. 47. 10.1002/cta.2694.
3. M. Arias, I. Castro, D. G. Lamar, A. Vázquez and J. Sebastián, "Optimized Design of a High Input-Voltage-Ripple-Rejection Converter for LED Lighting," in IEEE Transactions on Power Electronics, vol. 33, no. 6, pp.5192-5205, June 2018, doi: 10.1109/TPEL.2017.2727343.
4. Kim, Jong-Woo, Jung-Muk Choe, and Jih-Sheng Jason Lai. "Non-isolated single-switch two-channel LED driver with simple lossless snubber and low-voltage stress." IEEE Transactions on Power Electronics 33.5 (2017): 4306-4316.
5. V. K. S. Veeramallu, S. Porpandiselvi and B. L. Narasimharaju, "A Nonisolated Wide Input Series Resonant Converter for Automotive LED Lighting System," in IEEE Transactions on Power Electronics, vol. 36, no. 5, pp. 5686-5699, May 2021, doi: 10.1109/TPEL.2020.3032159
6. M. Khatua et al., "High-Performance Megahertz-Frequency Resonant DC–DC Converter for Automotive LED Driver Applications," in IEEE Transactions on Power Electronics, vol. 35, no. 10, pp. 10396-10412, Oct. 2020.

7. A. Agrawal, K. C. Jana and A. Shrivastava, “A review of different DC/DC converters for power quality improvement in LED lighting load,” 2015 International Conference on Energy Economics and Environment (ICEEE), 2015, pp. 1-6.
8. V. C. Bender, T. B. Marchesan and J. M. Alonso, "Solid-State Lighting: A Concise Review of the State of the Art on LED and OLED Modeling," in IEEE Industrial Electronics Magazine, vol. 9, no. 2, pp. 6-16, June 2015.
9. Y. Wang, J. M. Alonso and X. Ruan, "A Review of LED Drivers and Related Technologies," in IEEE Transactions on Industrial Electronics, vol. 64, no. 7, pp. 5754-5765, July 2017.
10. S. Li, S. -C. Tan, C. K. Lee, E. Waffenschmidt, S. Y. Hui and C. K. Tse, “A survey, classification, and critical review of light-emitting diode drivers,” IEEE Transactions on Power Electronics, vol. 31, no. 2, pp. 1503-1516, Feb. 2016.
11. Pollock, A., Pollock, H., Pollock, C.: ‘High Efficiency LED Power Supply’, IEEE Journal of Emerging and Selected Topics in Power Electronics, 2015, 3, (3), pp. 617-623
12. Yu, W., Lai, J. S., Ma, H., Zheng, C.: ‘High-Efficiency DC–DC Converter With Twin Bus for Dimmable LED Lighting’, IEEE Transactions on Power Electronics, 2011, 26, (8), pp. 2095-2100
13. Garcia, J., Calleja, A. J., Corominas, E. L., et al.: ‘Interleaved Buck Converter for Fast PWM Dimming of High-Brightness LEDs’, IEEE Transactions on Power Electronics, 2011, 26, (9), pp. 2627-2636
14. Mounika D, Vishwanathan N & Porpandiselvi S (2020): A level shifted asymmetric duty cycle controlled half-bridge series resonant LED driver configuration, EPE Journal, DOI: 10.1080/09398368.2020.1725858
15. H. R. Kolla, N. Vishwanathan and B. K. Murthy, "Independently Controllable Dual-Output Half-Bridge Series Resonant Converter for LED Driver Application," in IEEE Journal of Emerging and Selected Topics in Power Electronics, vol. 10, no. 2, pp. 2178-2189, April 2022.
16. R. R. Udumula, M. Vijayan, C. K. R. Reddy, M. Syed, A. Patakamoori and B. Gopichand, "A Three Leg Asymmetrical Voltage Resonant Converter with Independent Dimming Control for Multiple Load LED Lighting Applications," in IEEE Transactions on Industry Applications, doi: 10.1109/TIA.2024.3363676.
17. H. R. Kolla, N. Vishwanathan, and B. K. Murthy, “Input voltage controlled full-bridge series resonant converter for led driver application,” IET Power Electronics, vol. 13, DOI 10.1049/iet-pel.2020.0554, no.19, p.4532-4541, Dec. 2020.
18. C. Kasi Ramakrishnareddy, S. Porpandiselvi, and N. Vishwanathan, “Soft switched full-bridge light emitting diode driver configuration for street lighting application,” IET Power Electronics, vol. 11, DOI 10.1049/ietpel.2017.0021, no. 1, pp. 149–159, 2018.
19. V. K. S. Veeramallu, P. S., and N. B. L., “A buck-boost integrated high gain non-isolated half-bridge series resonant converter for solar pv/battery fed multiple load led lighting applications,” International Journal of Circuit Theory and Applications, vol. 48, pp. 266–285, 2020.
20. U. Ramanjaneya Reddy and B. L. Narasimharaju, “A cost-effective zero-voltage switching dual-output led driver,” IEEE Transactions on Power Electronics, vol. 32, DOI 10.1109/TPEL.2016.2636244, no. 10, pp. 7941– 7953, Oct. 2017.
21. J. M. Alonso, M. S. Perdigão, M. A. Dalla Costa, G. Martínez and R. Osorio, "Analysis and Experiments on a Single-Inductor Half-Bridge LED Driver With Magnetic Control," in IEEE Transactions on Power Electronics, vol. 32, no. 12, pp. 9179-9190, Dec. 2017.
22. K. R. Ch, S. Porpandiselvi, and N. Vishwanathan, “A three-leg resonant converter for two output led lighting application with independent control,” International Journal of Circuit Theory and Applications, vol. 47, DOI 10.1002/cta.2632, no. 7, pp.1173-1187.
23. J. Ribas, P. J. Quintana-Barcia, J. Cardesin, A. J. Calleja and E. L. Corominas, "LED Series Current Regulator Based on a Modified Class-E Resonant Inverter," in IEEE Transactions on Industrial Electronics, vol. 65, no. 12, pp. 9488-9497, Dec. 2018.
24. Rodrigues, W. A., Morais, L. M. F., Donoso-Garcia, P. F., et al.: ‘Comparative analysis of power LEDs dimming methods’, XI Brazilian Power Electronics Conference, Praiamar, 2011, pp. 378-383.